HYPERSPECTRAL BAND SELECTION BASED ON ENDMEMBER DISSIMILARITY FOR HYPERSPECTRAL UNMIXING

Mingming Xu[1], Yuxiang Zhang[2], Jie Li[3], Jiayi Li[4], Dongmei Song[1], Yanguo Fan[1], and Ning Sun[1]

1. School of Geosciences, China University of Petroleum (East China), P.R. China.
2. Institute of Geophysics and Geomatics, China University of Geosciences, P.R. China.
3. School of Geodesy and Geomatics, Wuhan University, P.R. China.
4. School of Remote Sensing and Information Engineering, Wuhan University, P.R. China.

ABSTRACT

Hyperspectral remote sensing could acquire hundreds of bands to cover a complete spectral interval, which deliver more information and allow a whole range of new and more precise applications. But vast data volume can cause trouble in computer processing and data transmission. Too many bands may cause interference for image processing and endmember variability is inevitable in hyperspectral data, which will affect the accuracy of interpretation. Band selection for hyperspectral image data is an effective way to mitigate the curse of dimensionality. In this paper, one hyperspectral band selection method based on endmember dissimilarity is proposed. This method used Mahalanobis distance as class separability criterion, and the spectral signature for each class is proposed by endmember extraction method automatically. Experiments on both synthetic and real hyperspectral data sets indicate that the proposed method outperformed the Minimum Estimated Abundance Covariance (MEAC) and Uniform Spectral Spacing (USS) method.

Index Terms— hyperspectral image, band selection, unmixing

1. INTRODUCTION

Dozens or hundreds of narrow, adjacent spectral bands represent unique material in hyperspectral remote sensing image. Due to more information contained in hyperspectral data, it allows a whole range of new and more precise applications. But, one question is whether all of the wavebands are actually necessary for a particular application. For example, one task to distinguish grass and water, red wavelengths and near infrared wavelengths is enough. Much more bands may interfere with the classification results. Secondly, when performing supervised classification, it is important that the number of training samples must larger than number of bands. It is often hard to attain when using hyperspectral data. Thirdly, neighboring bands in hyperspectral data are generally strongly correlated and some bands may contain less discriminatory information than others. At last, spectral variability which is inevitable in hyperspectral image will affect the accuracy of interpretation

Dimensionality reduction is one widely used way to overcome above problems. Methods of dimensionality reduction can be achieved by a transform-based approach, such as PCA, or a band-selection method. However, these transform-based methods usually change the physical meaning of the original data. Band-selection methods select a subset of the original bands without losing their physical meaning. In this paper, we limit the discussion on band selection.

Band selection can be either supervised or unsupervised. Supervised band selection can be seen as an optimization problem associated with some criteria, such as a class separability measure [1]–[3]. It only works when the the class knowledge is known as a priori. However, in many real applications, there is often very little a priori knowledge available. Unsupervised band selection does not require a priori knowledge. They usually rely on the basic idea of finding the most informative bands that are distinctive from others [4]–[6]. Discrimination criteria in unsupervised band selection methods were commonly universal, but it maybe not the best choice for a certain task.

In this paper, we proposed a band selection method based on endmember dissimilarity. It is a supervised band selection method without any priori. This method used Mahalanobis distance as class separability criterion, and the spectral signature for each class is proposed by endmember extraction method automatically. What is more, through the final results, we also could estimate the number of endmembers accurately.

The rest of the paper is organized as follows. Section II describes a band selection method based on endmember dissimilarity. Section III presents a comparison of proposed method, MEAC and USS with both simulated and real data sets. Section IV concludes the paper and introduces the future research.

2. METHOD

In this section, a band selection method based on endmember dissimilarity is described detailed. In order to select the most distinctive and informative bands, water absorption and low SNR bands need to be preremoved. This is because they can be very distinctive but not informative.

A. Endmember extraction

In a supervised band selection where class signatures are known, band-selection process can be greatly simplified. If there is no priori information, endmember extraction method can be used for class signatures extraction. In this paper, VCA is used for endmember extraction [8]. It also can be replaced by other endmember extraction methods [9][10].

VCA algorithm models the data as a positive cone, whose projection onto a properly chosen hyperplane is a simplex, with vertices being the endmembers. After projecting the data onto the selected hyperplane, then projects all the pixels to a random direction and uses the pixel with the largest projection as the first endmember. The other endmembers are identified by iteratively projecting the data onto a direction orthogonal to the subspace spanned by the endmembers already determined. The new endmember is then selected as the pixel corresponding to the extreme projection.

For VCA methods, the number of endmember should be known in advance. In experiments, we set an initial number and make adjustments according to the results. Details will be discussed in the experiments part.

B. Band selection method based on endmember dissimilarity

In order to select the most dissimilar bands, a similarity metric needs to be designated. The widely used metrics include distance, correlation, etc. Endmember dissimilarity based on Mahalanobis distance is used here.

Assume that there are p classes present in an image scene. Let the endmember matrix extracted by VCA be $S = [s_1, s_2, ..., s_p]$, then the endmember dissimilarity function can be defined as [11]:

$$g(S) = \frac{2}{p(p-1)} \sum_{i=1}^{p-1} \sum_{j=i+1}^{p} D(s_i, s_j) \quad (1)$$

where $D(s_i, s_j)$ means the Mahalanobis distance between s_i, s_j :

$$D(s_i, s_j) = \sqrt{(s_i - s_j)^{\mathrm{T}} \Sigma^{-1}(s_i - s_j)} \quad i \neq j \quad (2)$$

where Σ is the covariance of whole data.

The Mahalanobis distance is a measure of the distance between a point P and a distribution D, introduced by P. C. Mahalanobis [12]. It is also effective to calculate the similarity between two points under the same distribution. Unlike Euclidean distance, it considers the influence of overall variation (variance), and scale independent.

The proposed method's basic steps can be described as follows:

1) Calculate $g_i(S)$ $i = 1, 2, ..., L$ using each band, and L is the number of bands.

2) The first selected band $\Phi_1^S = \{Bl\}$:

$$Bl = \arg\max_{B_i} (g_i(S)) \quad i = 1, 2, ..., L \quad (3)$$

3) Calculate $g_i(S)$ using $\Phi^{S_i} = \{\Phi_1^S, B_i\}$ $i = 1, 2, ..., L$ *and* $i \neq Bl$, and L is the number of bands. The first selected band $\Phi_2^S = \{Bl, B2\}$ according to Eq. (3).

4) Repeat step 3) until the desired number of bands has been added to Φ.

From the above flow, we can see that this method does not need a large number of training samples; does not need to do classification to each combination, and there's no need to separate the initial band selection. We only need the spectral information that can be extracted by the endmember extraction algorithm.

3. EXPERIMENT

This section describes the experiments conducted on both simulated and real hyperspectral data, to allow a comprehensive analysis of the proposed method compared with USS and MEAC. Because we cannot obtain enough training samples to calculate statistics of each class, JM-based method and Bhattacharyya-distance-based method cannot achieve well results, which are not used here. What is more, unmixing results were used to evaluate band selection results.

The RMSE metric, which is widely used in the study of hyperspectral unmixing, is used to evaluate the unmixing results. Because all the endmembers and the corresponding abundances in the simulated image are known in advance, root-mean-square error (RMSE) is taken to evaluate the similarity of true versus estimated abundances:

$$RMSE_{i,j} = (\frac{1}{p}(a_{i,j} - \hat{a}_{i,j})^{\mathrm{T}}(a_{i,j} - \hat{a}_{i,j}))^{\frac{1}{2}}$$

$$\overline{RMSE}_{abundance} = \frac{1}{L} \sum \sum RMSE_{i,j} \quad (4)$$

where: p is the number of endmembers, L is the number of pixels.

In real data experiments, we do not know the true abundances in advance, so the difference of image versus reconstructed image is used to evaluate, which is also named RMSE:

$$RMSE_{i,j} = (\frac{1}{B}(S\hat{a}_{i,j} - y_{i,j})^{\mathrm{T}}(S\hat{a}_{i,j} - y_{i,j}))^{\frac{1}{2}}$$

$$\overline{RMSE}_{reconstruction} = \frac{1}{L} \sum \sum RMSE_{i,j} \quad (5)$$

where: B is the number of bands; L is the number of pixels; y is spectrum in image data.

A. Synthetic Hyperspectral Image

In this experiment, we derive a subset of six endmembers from the USGS spectral library [13] (shown in fig. 1) and use them to generate a simulated hyperspectral image with

100×100 pixels covering 224 bands. The abundance maps are illustrated in Fig. 2. There are pure pixels regions as well as mixed pixel regions. The synthetic hyperspectral image is implanted with noise (SNR=40).
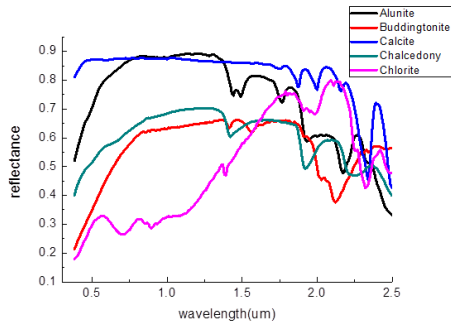
Fig. 1 Six endmembers from the USGS spectral library
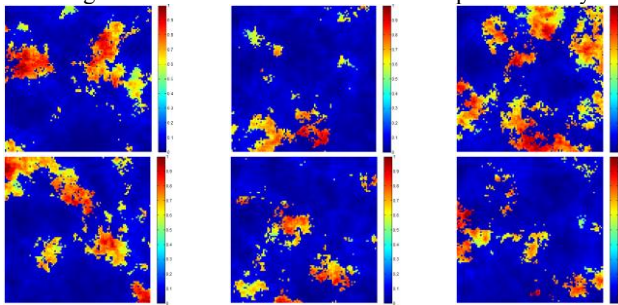
Fig. 2 Abundance maps for the series of simulated scenes

1) the number of endmembers analysis

In synthetic hyperspectral image, there are 6 endmembers. We tested how the endmember dissimilarity function $g(S)$ changed with the number of bands selected increase when the number of endmembers is set blow or above 6 (shown in fig. 3).
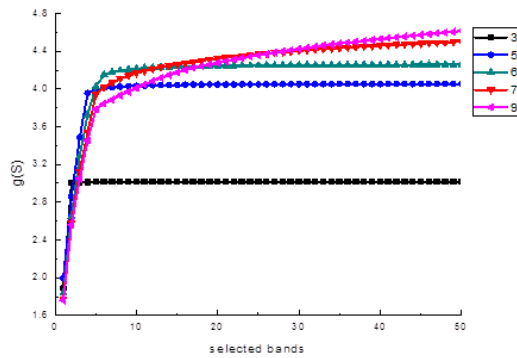
Fig. 3 the number of endmembers analysis

From fig. 3, we can see that: 1) If the number of endmembers in VCA is less than or equal to the real value, g(S) tend to be stable after a certain point; 2) If the number of endmembers in VCA is larger than the real number, g(S) will always increase after the certain point (the number of endmembers) at the speed of visible growth.

2) Unmixing results

Unmixing results were used to evaluate band selection results. And the number of selected bands changed from the number of endmembers to 50. Unmixing results using different bands are shown in fig.4. From fig.4, we can see that the proposed method outperformed the MEAC and USS with the smallest RMSE using 10bands and 25bands. What is more, the number of endmember is not the best number of bands to choose.
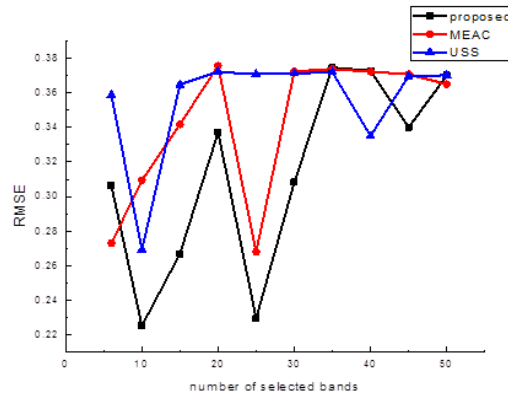
Fig. 4 Comparison between proposed method and MEAC, USS on unmixing accuracy

B. Real Data

The real data set covering the Cuprite scene was captured by AVIRIS (Airborne Visible Infrared Imaging Spectrometer), and is shown in Fig. 5. There are 182 bands in the data, with a size of 250×190, covering the wavelength range of 0.5−2.5 μm. The data set has become a popular benchmarking data set for algorithm evaluation, due to the extensive ground truth spectra available for the scene from the USGS.

Fig. 5. The AVIRIS Cuprite subscene

1) the number of endmembers analysis

In real hyperspectral image, we do not know the number of endmembers. The number of endmembers is changed from 10 to 20 in experiments to get different g(S) curves under different endmember numbers. Five representative curves are shown in fig. 6. According to the conclusion in above experiments about endmember number analysis, the number of endmembers in real data is determined to 14. Because when the number of endmembers set is larger than the real

number, the value of g(S) will always increase after the certain point (the number of endmembers) at the speed of visible growth.
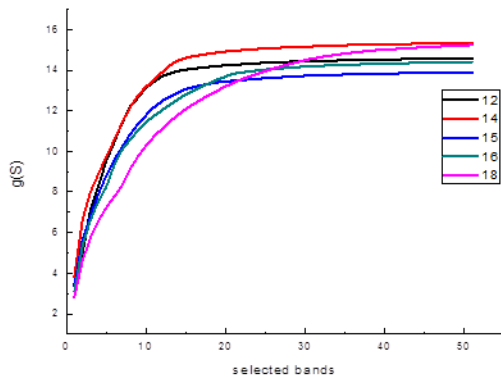
Fig. 6. The number of endmembers analysis

2) Unmixing results

The number of selected bands changed from the number of endmembers 14 to 50. Unmixing results with different bands are shown in fig.7. From fig.7, we can see that the proposed method outperformed the MEAC and USS with the smallest RMSE using 25bands. It is strange that there is no rule for the line chart in fig.7.
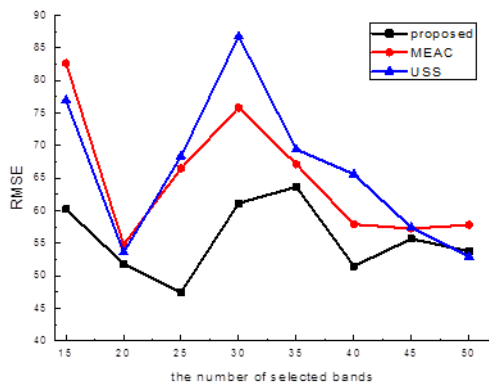
Fig. 7 Comparison between proposed method and MEAC, USS on unmixing accuracy

4. CONCLUSION

We developed new supervised band selection algorithms for hyperspectral imagery. The major contributions are the following: 1) employing the ideas of endmember dissimilarity as measurement without any priori; 2) from the endmember dissimilarity function curves we also could estimate the number of endmembers.

5. ACKNOWLEDGMENTS

6. REFERENCES

[1] Q. Du and H. Yang, "Similarity-based unsupervised band selection for hyperspectral image analysis," IEEE Geosci. Remote Sens. Lett., vol. 5, no. 4, pp. 564–568, Oct. 2008.

[2] W. Xia, B. Wang, and L. Zhang, "Band selection for hyperspectral imagery: A new approach based on complex networks," IEEE Geosci. Remote Sens. Lett., vol. 10, no. 5, pp. 1229–1233, Sep. 2013.

[3] S. S. Shen and E. M. Bassett, "Information theory based band selection and utility evaluation for reflective spectray systems," Proc. SPIE, vol. 4725, pp. 18–29, 2002.

[4] H. Su, H. Yang, Q. Du, and Y. Sheng, "Semi-supervised band clustering for dimensionality reduction of hyperspectral imagery," IEEE Geosci. Remote Sens. Lett., vol. 8, no. 6, pp. 1135–1139, Nov. 2011.

[5] J. Yin, Y. Wang, and J. Hu, "A new dimensionality reduction algorithm for hyperspectral image using evolutionary strategy," IEEE Trans. Ind. Informat., vol. 8, no. 4, pp. 935–943, Nov. 2012.

[6] S. Patra, P. Modi, and L. Bruzzone, "Hyperspectral band selection based on rough set," IEEE Trans. Geosci. Remote Sens., vol. 53, no. 10, pp. 5495–5503, Oct. 2015.

[7] H. Yang, Q. Du, H. Su, and Y. Sheng, "An efficient method for supervised hyperspectral band selection," IEEE Geosci. Remote Sens. Lett., vol. 8, no. 1, pp. 138–142, Jan. 2011.

[8] J. Nascimento and J. Bioucas-Dias, "Vertex component analysis: A fast algorithm to unmix hyperspectral data," IEEE Trans. Geosci. Remote Sens., vol. 43, no. 4, pp. 898–910, 2005.

[9] L. Wang, F. Wei, D. Liu, and Q. Wang, "Fast Implementation of Maximum Simplex Volume-Based Endmember Extraction in Original Hyperspectral Data Space," IEEE J. Sel. Topics Appl. Earth Observ., vol. 6, pp. 516-521, 2013.

[10] X. Geng, L. Ji, F. Wang, Y. Zhao, and P. Gong, "Statistical Volume Analysis: A New Endmember Extraction Method for Multi/Hyperspectral Imagery," IEEE Trans. Geosci. Remote Sens., vol. 54, pp. 6100-6109, 2016.

[11] N. Wang, B. Du, L. Zhang, "An endmember dissimilarity constrained non-negative matrix factorization method for hyperspectral unmixing," IEEE J. Sel. Topics Appl. Earth Observ. , vol. 6, no. 2, pp. 554-569, 2013.

[12] P. C. Mahalanobis, "On the generalised distance in statistics," Proceedings of the National Institute of Science of India, 1936, 12: 49-55.

[13] R. N. Clark, G. A. Swayze, A. Gallagher, T. V. King, and W. M. Calvin, "The U.S. Geological Survey digital spectral library: Version 1: 0.2 to 3.0," U. S. Geological Survey, Open File Rep., pp. 93–592, 1993.